Photoinduced Birefringence and Surface Relief Gratings in Novel Polyurethanes with Azobenzene Groups in the Main Chain

Yiliang Wu,[†] Almeria Natansohn,*[,†] and Paul Rochon[‡]

Department of Chemistry, Queen's University, Kingston, Ontario, Canada K7L 3N6, and Department of Physics, Royal Military College, Kingston, Ontario, Canada K7K 5L0

Received February 13, 2001; Revised Manuscript Received August 21, 2001

ABSTRACT: Three novel polyurethanes with V-shaped bisazo groups (**PU1** and **PU2**) or rodlike monoazo groups (**PU3**) in the main chain were synthesized. On irradiation with a linearly polarized laser beam, birefringence was induced in the three films to the level of 0.035, 0.037, and 0.044 for **PU1**, **PU2**, and **PU3**, respectively. The stable birefringence obtained at $T_g - T = 33$ °C was 71%, 46%, and 19% of that achieved at room temperature for **PU1**, **PU2**, and **PU3**, respectively. The relative stability of the photoinduced birefringence of **PU3** decreased linearly with the increase of temperature, while that of **PU1** and **PU2** was constant even close to T_g. Surface relief gratings with high diffraction efficiency were inscribed on these main-chain polymers. The photoinduced gratings are only partially erasable by heating above the T_g of the polymers.

Introduction

Azobenzene and substituted azobenzenes have been known for a long time. In recent years, azobenzene-containing polymeric systems have been the subject of intensive research due to their unique and unexpected properties which allow various applications triggered by light.[1] One of the attractive phenomena is photoinduced dichroism and birefringence in films when illuminated with linearly polarized light. Also, massive movement of the polymer material, creating micrometer-deep surface relief gratings, was observed by exposing the polymer film to interfering laser beams.[2,3]

The azo-containing polymer literature is huge; some studies include polymer matrices doped with azo dyes,[4] liquid-crystalline azo polymers,[5−7] Langmuir−Blodgett films,[8,9] and amorphous azo polymers.[10,11] Previous studies in this laboratory demonstrated that an efficient optical response could be induced in amorphous polymers with relatively high glass transition temperatures (T_g).[10,11] The azobenzene groups are attached to the polymer main chain directly or through flexible spacer.[11] Variable temperature studies showed that orientation could be achieved even close to T_g in the amorphous polymers, but it is not stable, because of a significant degree of motion in the film at these temperatures, which restores disorder.[12,13] More recently, photoinduced birefringence and surface relief gratings were investigated at room temperature in polyesters and in high-T_g polyureas with azobenzene units in the main chain.[14−16]

The stability of the optically induced birefringence and the magnitude of surface relief gratings are strongly associated with polymer properties such as the chromophore structure, the rigidity of polymer main chain, and the interaction between chromophore and the main chain. For example, highly stable photoinduced birefringence was achieved in an azocarbazole-based polyimide.[17] To increase the stability of the photoinduced birefringence and to generate high efficient surface relief gratings, new azo polymers are being designed and synthesized. Polyurethanes bearing azo chromophores in the main chain have been studied earlier for use in nonlinear optics.[18,19] Long-term and high-temperature stability of the second-order nonlinear optical effects was reported. In this study, three novel polyurethanes containing donor−acceptor type azobenzene groups in the main chain are presented (Scheme 1). The azo chromophores are a V-shaped bisazo and a common rodlike monoazo (Scheme 2).

Experimental Section

Materials. 4-Aminophenyl sulfone, 2-(*N*-ethylanilino)ethanol, 1,4-phenylene diisocyanate (1,4-PDI), 2,4-tolylene diisocyanate (2,4-TDI), and the polymerization solvent *N*,*N*-dimethylformamide (DMF, 99.8%, anhydrous) were received from Aldrich Chemical Co. and used without further purification.

Chemical Characterization. ^{1}H NMR spectra were recorded on a Bruker AVANCE 300 MHz NMR spectrometer in $CDCl_3$ or DMSO-d_6. UV−vis spectra were recorded on a Hewlett-Packard UV−vis spectrometer in solid film and in DMF at room temperature. Gel permeation chromatography (GPC) analysis was performed on a Water Associates liquid chromatograph equipped with a model R401 differential refractometer using polystyrene as standards. Differential scanning calorimetry (DSC) measurements were done on a Perkin-Elmer DSC-6 under nitrogen atmosphere using a heating rate of 20 °C/min.

Monomers. The bisazo-diol monomer, ((((2-hydroxyethyl)-ethylamino)phenyl)diazenyl)phenyl sulfone, was synthesized by diazotization reaction and followed by coupling with aniline (Scheme 1). 4-Aminophenyl sulfone (5 g, 20.2 mmol) was dissolved in 50 mL of glacial acetic acid containing 9 mL of concentrated HCl. The temperature was maintained at 0−5 °C. Sodium nitrite (3.1 g, 44.9 mmol) dissolved in a small amount of water was added dropwise to the stirred solution. The reaction was allowed at 5 °C for 2 h. 2-(*N*-Ethylanilino)-ethanol (6.7 g, 40.6 mmol) and sodium acetate (5 g, 61 mmol) in 50 mL of acetic acid were added slowly. The resulted red solution was stirred for 4 h at 0−5 °C and for an additional 16 h at room temperature. Sodium hydroxide solution was slowly added to neutralize the reaction mixture. The precipitate formed was collected by filtration, washed with a large amount of water, and dried. The crude products were purified by column chromatography using 3% methanol in chloroform

[†] Queen's University.
[‡] Royal Military College.
* Corresponding author.

10.1021/ma0102722 CCC: $20.00
Published on Web 09/26/2001

Scheme 1

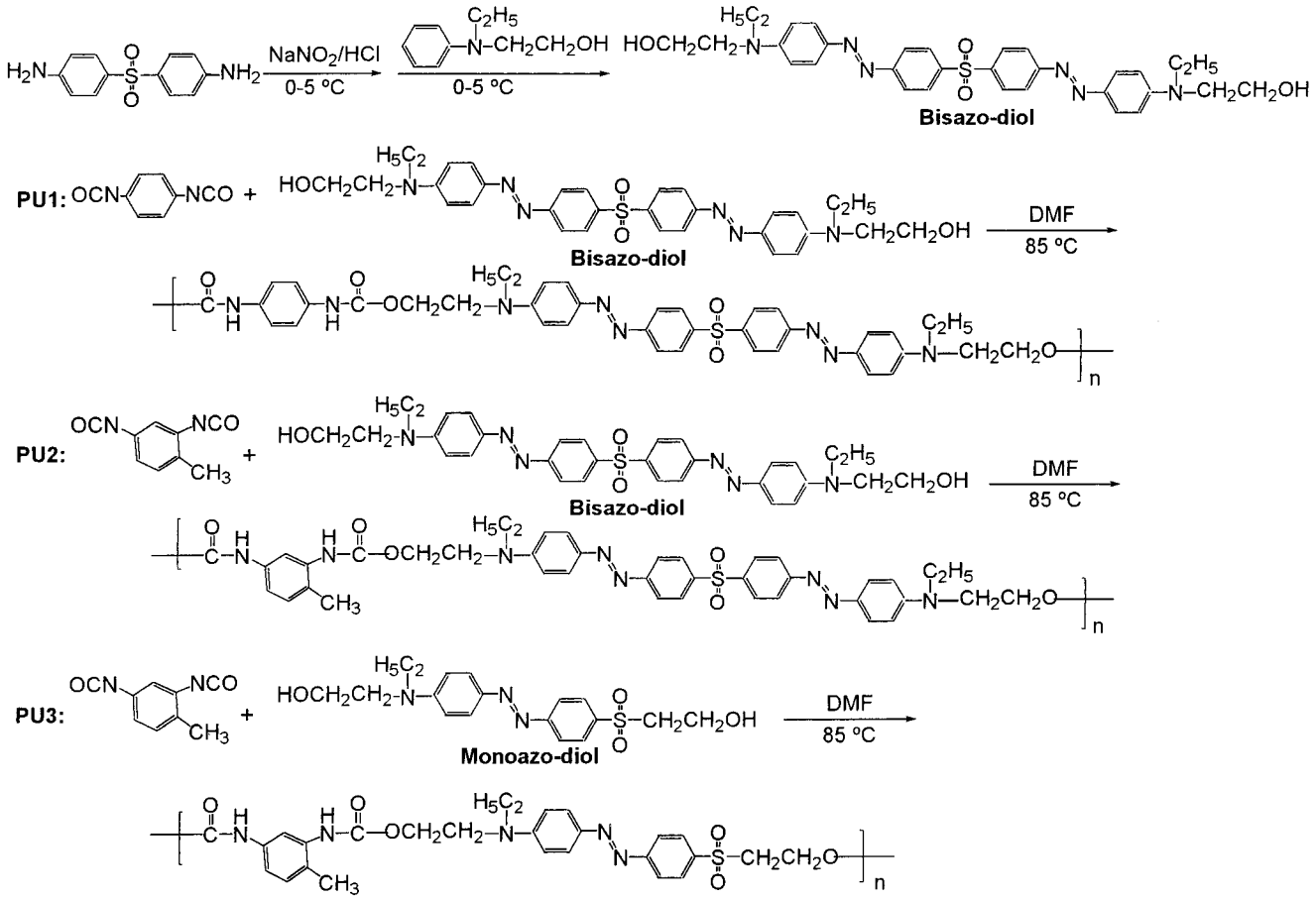

Scheme 2

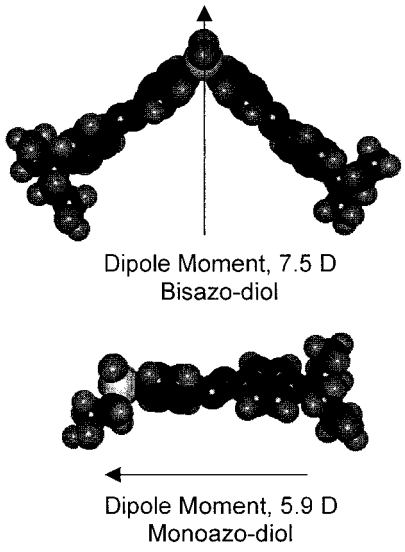

as eluent to afford pure bisazo-diol monomer (7.6 g, 63%). ^{1}H NMR ($CDCl_3$): δ (ppm) 8.05 (d, 4 aromatic H, ortho to $-SO_2-$), 7.8−7.95 (2d, 8 aromatic H, ortho to $-N{=}N-$), 6.81 (d, 4 aromatic H, ortho to $-N-$), 3.89 (m, 4H, $-CH_2-OH$), 3.50−3.66 (m, 8H, $-CH_2-N$), 1.76 (s, 2H, $-OH$), 1.25 (t, 6H, $-CH_3$). UV: $\lambda_{max} = 482$ nm.

The monoazo-diol, 4-((2-hydroxyethyl)ethylamino)-4′-(2-hydroxyethylsulfonyl)azobenzene, was synthesized as reported previously.[16,18] UV: $\lambda_{max} = 464$ nm.

Polymerization. Polyurethanes were synthesized by means of polyaddition reaction between diisocyanate and diol monomers under an argon atmosphere (Scheme 1). The reaction medium was heated at 85 °C for 48 h, cooled to room temperature, and then poured into 400 mL of vigorously stirred methanol. The resulting polymers were collected and purified by reprecipitation from methanol again and dried to a constant weight.

^{1}NMR (DMSO-d_6) of **PU1**: δ (ppm) 9.55 (2 H, $-CO-NH$), 8.1 (4 aromatic H, ortho to $-SO_2-$), 7.9 (4 aromatic H, meto to $-SO_2-$), 7.8 (4 aromatic H, meto to $-N-CH_2CH_2$), 7.3 (4 aromatic H, ortho to $-HN-CO$), 6.85 (4 aromatic H, ortho to $-N-CH_2CH_2$), 4.25 (4 H, $COO-CH_2-$), 3.7 (4 H, CH_2CH_2-N), 3.5 (4 H, $N-CH_2CH_3$), 1.15 (6 H, CH_3).

^{1}NMR (DMSO-d_6) of **PU2**: δ (ppm) 9.6 (1 H in $CO-NH$, ortho to CH_3), 8.8 (1 H in $CO-NH$, para to CH_3), 8.1 (4 aromatic H, ortho to $-SO_2-$), 7.9 (4 aromatic H, meto to $-SO_2-$), 7.8 (4 aromatic H, meto to $-N-CH_2CH_2$), 7.5 (1 aromatic H, ortho to both NHCO), 7.15 (1 aromatic H, meto to NHCO), 7.05 (1 aromatic H, ortho to CH_3), 6.85 (4 aromatic H, ortho to $-N-CH_2CH_2$), 4.25 (4 H, $COO-CH_2-$), 3.7 (4 H, CH_2CH_2-N), 3.5 (4 H, $N-CH_2CH_3$), 2.05 (3 H, ph-CH_3) 1.15 (6 H, CH_2CH_3).

^{1}NMR (DMSO-d_6) of **PU3**: δ (ppm) 9.55 (1 H in $CO-NH$, ortho to CH_3), 8.4−8.9 (1 H in $CO-NH$, para to CH_3), 8.05 (2 aromatic H, ortho to $-SO_2$-), 7.9 (2 aromatic H, meto to-SO_2-), 7.8 (2 aromatic H, meto to $-N-CH_2CH_2$), 7.45 (1 aromatic H, ortho to both NHCO), 7.15 (1 aromatic H, meto to NHCO), 7.05 (1 aromatic H, ortho to CH_3), 6.85 (2 aromatic H, ortho to $-N-CH_2CH_2$), 4.2−4.4 (4 H, $COO-CH_2-$), 3.6−3.9 (4 H, CH_2CH_2-N and $-CH_2-SO_2$), 3.5 (2 H, $N-CH_2CH_3$), 2.05 (3 H, ph-CH_3) 1.15 (3 H, CH_2CH_3).

Film Preparation and Optical Characterization. Thin films of the polyurethanes were obtained by dissolving the polymers in DMF. The solution were filtered with 0.45 μm syringe filters and then spin-coated onto clear glass substrates. The films were allowed to dry and subsequently heated in a vacuum oven at 70 °C for 24 h. Thickness of the films was measured by ellipsometry. Homogeneous films with a thickness from 100 to 200 nm for birefringence measurements and

Table 1. Properties of the Polymers

polymer	yield (%)	M_n	M_w/M_n	T_g (°C)	T_d (°C)[a]
PU1	82	17 000	2.2	182	285
PU2	77	22 000	2.1	167	260
PU3	91	10 000	1.9	143	240

[a] Onset decomposition temperature under nitrogen atmosphere.

around 350 nm for surface relief grating measurement were obtained.

The procedure for measuring the optically induced and erased birefringence has been previously described.[20] An argon laser (488 nm) with an irradiance of 65 mW/cm^2 was used as the light source. The birefringence was detected using a diode laser beam at 674 nm as a probe. Experiments were performed at various temperatures with an Instec temperature controller and heating stage to maintain temperatures accurate to within ±0.1 °C. Surface profile gratings were inscribed at room temperature using the co- and contra-circularly interfering beams. Details about the optical setup can be found elsewhere.[2,21] The dynamic diffraction efficiencies of the positive first order were measured on the 1 μm spacing grating with a time resolution of 1 point/s. The surface relief characteristics have been checked with atomic force microscopy.

Results and Discussion

Monomers and Polymers. We chose amine as the donor group because of its strong electron donor ability. Sulfone was used as the electron acceptor group since it is convenient to incorporate this group into the polymer main chain. The three-dimensional structure of the aromatic azo diols was calculated using Hyperchem software. As shown in Scheme 2, the monoazo-diol shows the common rodlike shape with a dipole moment of 5.9 D, while the bisazo-diol has a bent shape and a larger (7.5 D) dipole moment with a different orientation. The angle between the two halves of the molecule is 99.5°. Although the electron donor and acceptor groups are the same for both azo diols, due to the different molecular shapes, the value and orientation of the overall dipole moments are different, and so are the absorption maxima in UV−vis spectra.

Polyurethanes were prepared using commercial diisocyanates and the synthesized azo diols. **PU1** and **PU2** have the same V-shaped diazo chromophore but different isocyanate groups (1,4-PDI in **PU1**, 2,4-TDI in **PU2**). **PU3** has the same diisocyanate unit (2,4-TDI) as **PU2**, but a different rodlike monoazo chromophore. The polymers are easily soluble in DMF at room temperature. **PU1** and **PU2** are partially soluble in THF, while **PU3** is easily soluble. As summarized in Table 1, the main-chain azopolymers have relatively high T_g's. **PU3** has the lowest T_g among the three polymers. Incorporation of the rigid and bulky bisazo-diol increases the T_g. The glass transition temperature increases to 182 °C when 1,4-PDI is used instead of 2,4-TDI, probably because the methyl group in 2,4-TDI needs a larger free volume and the polymer chain may be less compact. The decomposition temperatures (the onset points at which the sample starts exothermal decomposition) show the same tendency as the T_g's. Figure 1 shows the UV−vis spectra of the polyurethane films. Absorption maxima are at 454, 448, and 442 nm for **PU1**, **PU2**, and **PU3**, respectively, assigned to the $\pi-\pi^*$ transition of the azobenzene chromophores.

Photoinduced Birefringence. Optically induced birefringence was investigated by exposing the polymer films to a linearly polarized laser beam at 488 nm. Figure 2 shows typical growth, relaxation, and elimination of the photoinduced birefringence in the polyurethane films. A photostationary birefringence of 0.044 can be induced in **PU3** by irradiation with the linearly polarized light. In comparison with the polyester having the same azobenzene group in the main chain,[16] the birefringence is lower, probably because of the higher molecular weight of **PU3**, which significantly increases the steric hindrance in a main-chain azo polymer. Birefringence is induced in the polyurethanes containing the bent shape bisazo groups as well. The photostationary values were observed to be 0.035 and 0.037 for **PU1** and **PU2**, respectively, which is smaller than, but still comparable with, that induced in **PU3**. The lower values are ascribed to the bent shape of the bisazo group, which is not favorable for birefringence. No significant difference was observed between **PU1** and **PU2**, although the diisocyanates were different. The birefringence could be completely eliminated by circularly polarized light and induced again by linearly polarized light.

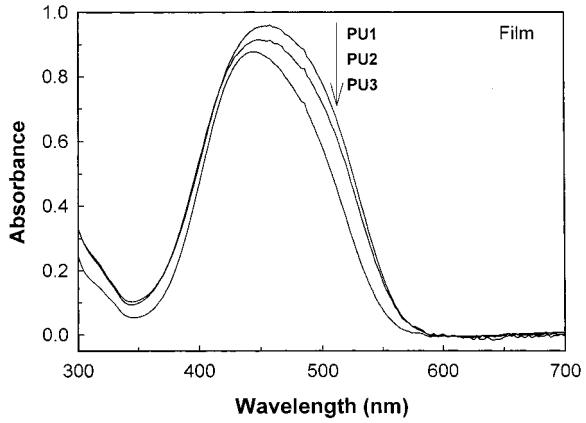

Figure 1. UV−vis spectra of the polyurethane films.

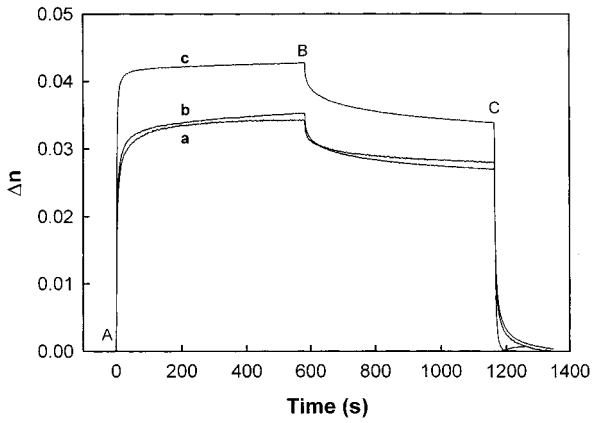

Figure 2. Typical birefringence curves for the polyurethane films. Linearly polarized light is turned on at point A and turned off at point B; circularly polarized light is turned on at point C. a, **PU1**; b, **PU2**, c, **PU3**.

Biexponential functions are used to describe the dynamics of growth and decay of the birefringence, with the assumption of two processes, a fast process and a slow one, to be responsible for the change of the birefringence.[22] The biexponential functions are

$$\Delta n = A\{1 - \exp(-k_a t)\} + B\{1 - \exp(-k_b)\}$$

for photoinducing birefringence and

$$\Delta n = C \exp(-k_c t) + D \exp(-k_d t) + E$$

Table 2. Kinetic Data for the Photoinduced Birefringence and the Dark Relaxation

polymer	A_n	B_n	k_a (s^{-1})	k_b (s^{-1})	C_n	D_n	E_n	k_c (s^{-1})	k_d (s^{-1})
PU1	0.82	0.18	0.264	0.023	0.09	0.10	0.81	0.094	0.004
PU2	0.82	0.18	0.286	0.011	0.11	0.14	0.75	0.078	0.004
PU3	0.95	0.05	0.330	0.008	0.08	0.12	0.80	0.075	0.004

for the relaxation process in the absence of illumination, where Δn is the birefringence observed at time t; k_a, k_b, k_c, and k_d represent the rate constants with the amplitudes (preexponential parameters) of A, B, C, and D, respectively. It is convenient to normalize the preexponential parameters; thus, A_n is defined as $A/(A + B)$, and C_n is defined as $C/(C + D + E)$, etc. E_n is the fraction of birefringence conserved for a very long time. The parameters obtained by fitting the curves in Figure 2 to the above two equations are summarized in Table 2. The rate constants of the fast growth process increase with the decrease of the T_g of the polymers. The relaxation rates and the stability of the photoinduced birefringence (E_n) are almost the same for the three samples.

Temperature Dependence. The temperature dependence of the photoinduced birefringence in side-chain azo polymers is relatively well understood.[12,13] Birefringence can be induced even close to T_g, but it is not stable, due to thermal motion. Photoinduced birefringence in the main-chain polyurethanes was studied at various temperatures. Figure 3 shows the photostationary (point B in Figure 2) and stable (point C in Figure 2) levels of the birefringence as a function of a reduced temperature. Similar to the side-chain azo polymers, both the photostationary and the stable values decrease with the increase of temperature. However, the decrease is different for the three polymers. The temperature effect is less pronounced in the polyurethanes with V-shaped chromophores. The stable birefringence obtained at $T_g - T = 33$ °C is 71%, 46%, and 19% of the room-temperature levels for **PU1**, **PU2**, and **PU3**, respectively.

In addition, the three polymers show different stability of the photoinduced birefringence as a function of temperature. As shown in Figure 3, the decrease of the stable birefringence is slower than the decrease of the photostationary value for **PU1** and **PU2**, while for **PU3** they are almost the same. In other words, the loss of birefringence from the photostationary state to the stable state decreases with the increase of temperature for **PU1** and **PU2**, while it stays constant for **PU3**. This produces a relatively high stability of the photoinduced birefringence at higher temperature for **PU1** and **PU2**. The stability, estimated by the parameter E_n, will be discussed in the following section.

It was reported that the rate constants of the photoinduced birefringence process decrease with the increase in temperature for one polymer containing donor−acceptor substituted azobenzenes in the side chain.[13] The polyurethanes investigated here exhibit a similar behavior (Figure 4). **PU3** shows the largest rate constants at all temperatures, probably due to the smaller sweep volume required by isomerization of the monoazo group and due to the higher flexibility of the polymer main chain. Although **PU1** and **PU2** have the same azobenzene group in the main chain, **PU2** exhibits larger rate constants. This may be because of the lower T_g and larger free volume of **PU2**, as mentioned above.

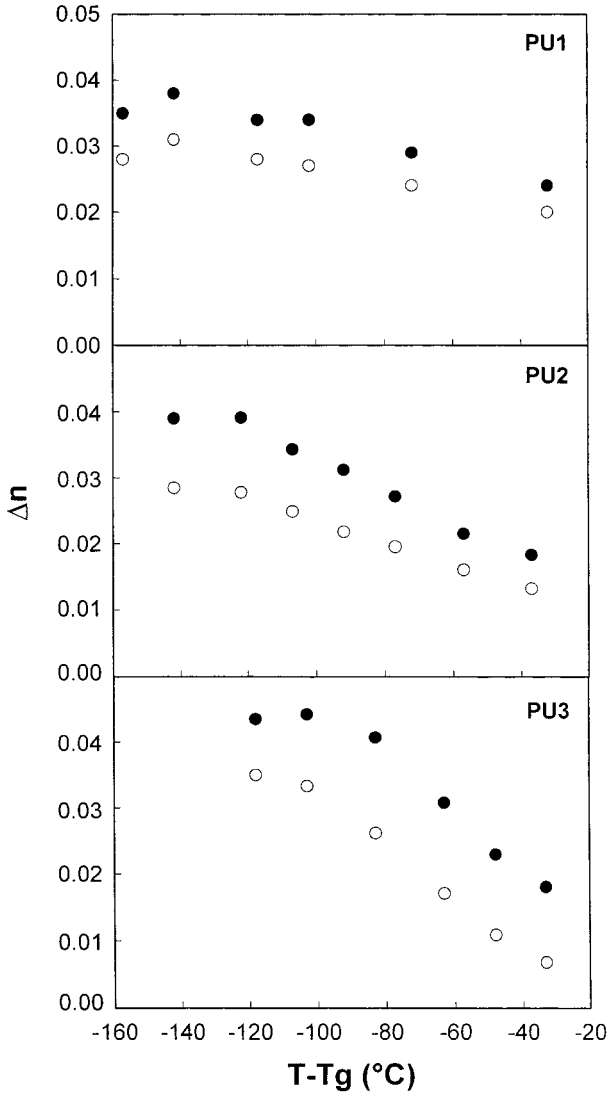

Figure 3. Photostationary (full circles) and stable (empty circles) levels of the photoinduced birefringence in polyurethanes as a function of reduced temperature.

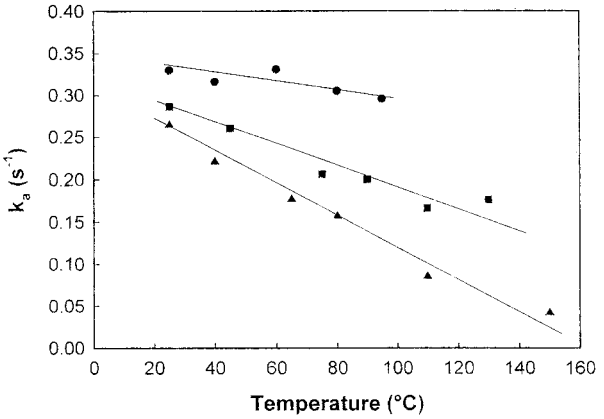

Figure 4. Rate constants of the fast growth process as a function of temperature. The lines are only guides for the eye. ▲, **PU1**; ■, **PU2**; ●, **PU3**.

The temperature effect on the rate constants increases with the increase of the polymers' T_g. In the case of **PU3**, which has the lowest T_g, the rate constants decrease slowly with the increase of temperature. However, in the case of **PU1**, with the highest T_g, the rate constants decrease quickly with the increase of temperature.

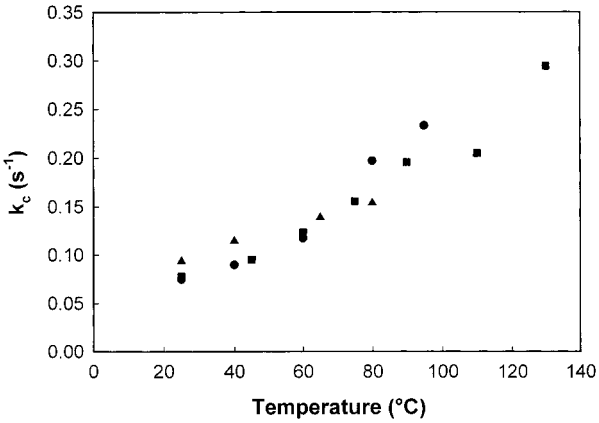

Figure 5. Rate constants of the fast relaxation process as a function of temperature. ▲, **PU1**; ■, **PU2**; ●, **PU3**.

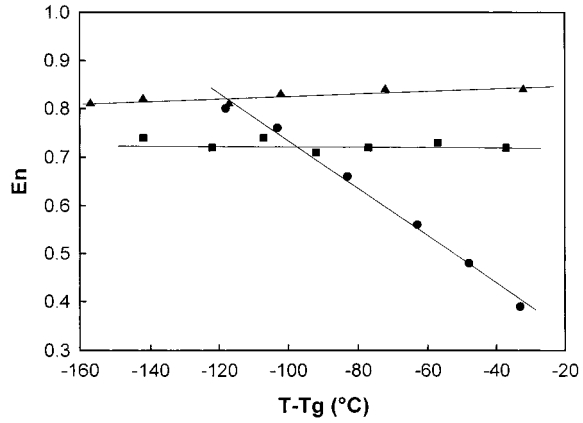

Figure 6. Long-term stable birefringence, E_n, as a function of reduced temperature. The lines are only guides for the eye. ▲, **PU1**; ■, **PU2**; ●, **PU3**.

Regarding the relaxation process, Figure 5 shows the fast relaxation constants as a function of temperature. The three polymers show almost the same rate constants at the same temperatures. With the increase in temperature, the rate constants increase. The fast relaxation process has the cis−trans thermal isomerization of the azobenzenes as the main component.[22] Therefore, the similar fast rate constants are probably due to similar cis−trans thermal isomerization rates of the bisazo and the monoazo groups, which have the same donor and acceptor groups. With the increase of temperature, the cis−trans isomerization rate of the azobenzene groups increases.

The most important parameter is E_n, which estimates the relative long-term stability of the photoinduced birefringence. Figure 6 shows the values of E_n of the polyurethanes as a function of the reduced temperature. With the increase of temperature, E_n of **PU3** decreased linearly. However, the relative stability of the photoinduced birefringence is constant for **PU1** and **PU2**, even at the temperatures close to T_g, although the photostationary and the stable values decrease with the increase of temperature. The behavior of **PU3** is very similar to that of other side-chain azo polymers;[12] thus, incorporation of the azobenzene chromophore into the polymer main chain does not increase the stability of the induced birefringence.

The fact that the birefringence induced in **PU1** and **PU2** at high temperatures shows a high relative stability might be explained by the following two reasons. First, the bulky bisazo group may improve the stability

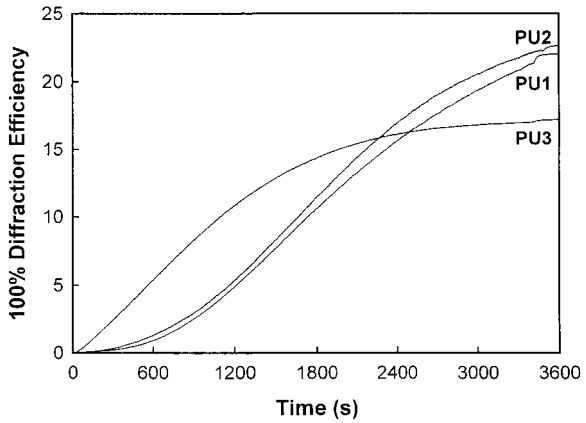

Figure 7. Diffraction efficiency of the surface gratings inscribed on the polyurethane thin films as a function of irradiation time. Irradiation light was turned on at 30 s and turned off at 3400 s. The film thickness is 360, 330, and 350 nm for **PU1**, **PU2**, and **PU3**, respectively.

of orientation. All experiments were conducted below T_g; thus, the effect of thermal motion on the bulky azobenzene groups in **PU1** and **PU2** is probably less important, even at high temperatures. Second, the special molecular shape of the bisazo groups might contribute to the high relative stability of the photoinduced birefringence. As illustrated in Scheme 2, the two azo moieties in the bisazo-diol are nearly perpendicular to each other. The relaxation of one azo moiety out of alignment might move the other moiety into the alignment direction. Future spectroscopic studies will address the orientation and relaxation behavior of the V-shaped bisazo groups in detail.

Optically Induced Surface Relief Gratings. Surface relief gratings have been inscribed on the three polyurethane films by the interference of left and right circularly polarized laser beams (488 nm, 250 mW/cm^2). Figure 7 shows the diffraction efficiency as a function of irradiation time. The diffraction efficiency is defined as the percentage of the first-order diffracted intensity with respect to the initial intensity of the probe light. Unlike the polyureas reported by Lee and co-workers,[14,15] high diffraction efficiencies were achieved in these main-chain azo polyurethanes, because they contain donor−acceptor substituted azobenzene chromophores. The values are comparable with those observed in side-chain azo polymers.[21] The diffraction efficiencies of **PU1** and **PU2** showed a similar behavior (typical S-type curve). Within the first 15 min, the diffraction efficiency increases very slowly. Then the increase accelerates, and the diffraction efficiency reaches a saturated value; however, the value is not reached within 1 h. In the case of **PU3**, the diffraction efficiency increases almost linearly with the irradiation time up to about 40 min, when a saturation value is reached.

Most surface relief gratings previously reported were thermally erasable. Permanent gratings were reported only on an azocarbazole-based polyimide[17] and on side-chain urethane−urea copolymers.[23] The polyimide did not show a T_g prior to thermal decomposition, while the urethane−urea copolymers underwent photobleaching. In this study, thermal erasing of the photoinduced surface relief gratings was carried out at 15 °C above the T_g of the polymers. The gratings could not be totally erased by heating. Figure 8 shows the normalized diffraction efficiency as a function of erasing time. Most of the decrease takes place within the first 15 min. After

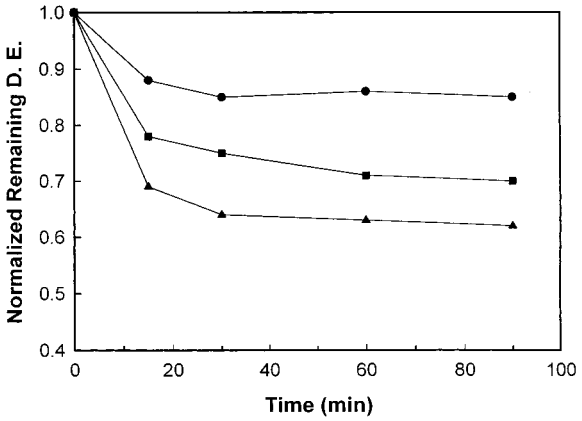

Figure 8. Normalized diffraction efficiency (DE) of the surface gratings inscribed on the polyurethane films as a function of erasing time. Thermal erasing was performed at 15 °C above the T_g of the polymers. ▲, **PU1**; ■, **PU2**; ●, **PU3**.

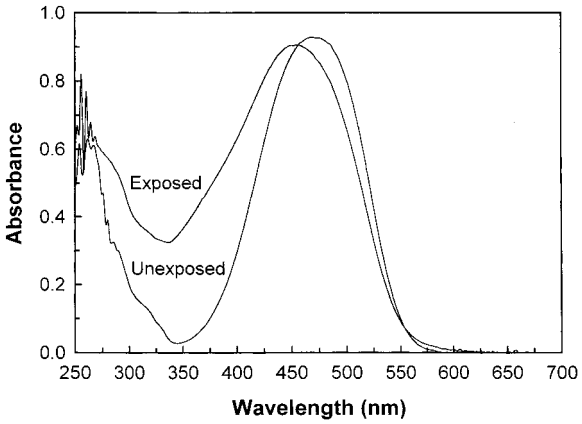

Figure 9. UV−vis spectra of **PU2** in DMF solution. The concentrations are different.

90 min, the remaining diffraction efficiency is about 60, 70, and 85% of the initial value for **PU1**, **PU2**, and **PU3**, respectively. Solubility tests showed that no significant cross-linking had occurred. After irradiation with the interfering laser beams for 55 min, the exposed and unexposed areas in **PU2** film were separately collected. UV−vis spectra were measured in DMF solution. As shown in Figure 9, the slight blue shift and strong absorption between 300 and 400 nm reveal that some photoreactions took place on irradiation of laser beam with this relatively high intensity (250 mW/cm^2). Therefore, the gratings still present after heating above T_g might be due to these irreversible photoreactions.

The surface relief is confirmed by using AFM. Figure 10 shows the images of **PU2** observed before and after thermal erasing. The gratings profile on the film surface exhibited a regularly sinusoidal shape with grating spacings of ~1 μm, as set by the interference pattern. Before erasing, the amplitude of the surface relief is around 300 nm; after thermal erasing a 260 nm amplitude remains. As expected, the thermal erasing process has no effect on the grating spacings. Table 3 summarizes the diffraction efficiencies and the amplitude of the surface relief grating before and after the thermal treatment for 90 min.

Conclusions

Three novel polyurethanes with amino-sulfone azobenzene chromophores in the main chain were synthesized. Optical studies showed that birefringence can be induced not only in the polyurethane having the common rodlike azobenzene units but also in the polyurethanes containing V-shaped bisazo units. Variable temperature studies showed that high levels as well as high relative stability of the induced birefringence could be obtained in **PU1** and **PU2** at relatively high temperatures. Surface relief gratings were inscribed on these main-chain polyurethanes. High diffraction efficiencies were observed even for the polymer with high T_g. The induced inscriptions are only partially erasable by thermal treatment.

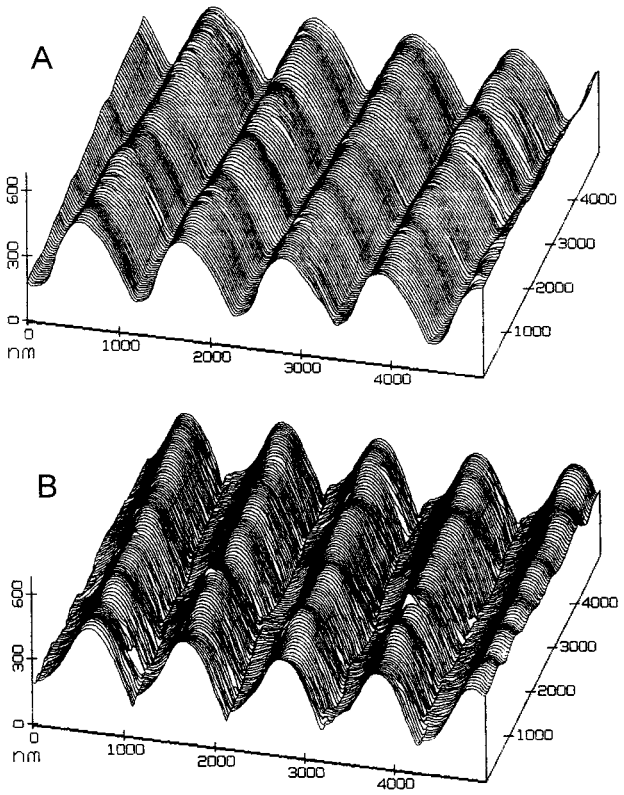

Figure 10. AFM surface grating profile of **PU2** observed before (A) and after (B) thermal treatment at 182 °C for 90 min.

Table 3. Diffraction Efficiency (DE) and Depth of Surface Relief Gratings before and after Thermal Erasing at $T = T_g + 15$ °C for 90 min

	before erasing		after erasing	
polymer	DE (%)	depth (nm)	DE (%)	depth (nm)
PU1	21.3	293	13.2	196
PU2	22.1	307	15.6	261
PU3	17.0	250	14.5	202

Acknowledgment. Funding from NSERC Canada and the Department of National Defence Canada is gratefully acknowledged. A.N., Canada Research Chair in Polymer Chemistry, thanks the CRC Program of the Government of Canada.

References and Notes

(1) Azobenzene-Containing Materials. *Macromolecular Symposia*; Natansohn, A., Ed.; Wiley-VCH Verlag: Weinheim, Germany, 1999; Vol. 137.

(2) Rochon, P.; Batalla, E.; Natansohn, A. *Appl. Phys. Lett.* **1995**, *66*, 136.

(3) Kim, D. Y.; Tripathy, S. K.; Li, L.; Kumar, J. *Appl. Phys. Lett.* **1995**, *66*, 1166.

(4) Todorov, T.; Nikolova, L.; Tomova, N. *Appl. Opt.* **1984**, *23*, 4309.
(5) Eich, M.; Wendorff, J. H.; Reck, B.; Ringsdorf, H. *Makromol. Chem., Rapid Commun.* **1987**, *8*, 59.
(6) Hvilsted, S.; Andruzzi, F.; Kulinna, C.; Siesler, H. W.; Ramanujam, P. S. *Macromolecules* **1995**, *28*, 2172.
(7) Wu, Y.; Demachi, Y.; Tsutsumi, O.; Kanazawa, A.; Shiono, T.; Ikeda, T. *Macromolecules* **1998**, *31*, 349.
(8) Ichimura, K. *Supramol. Sci.* **1996**, *3*, 67.
(9) Stumpe, J.; Fischer, Th.; Menzel, H. *Macromolecules* **1996**, *29*, 2831.
(10) Natansohn, A.; Rochon, P.; Gosselin, J.; Xie, S. *Macromolecules* **1992**, *25*, 2268.
(11) Natansohn, A.; Rochon, P. *Adv. Mater.* **1999**, *11*, 1387.
(12) Meng, X.; Natansohn, A.; Rochon, P. *J. Polym. Sci., Part B: Polym. Phys.* **1996**, *34*, 1461.
(13) Hore, D.; Natansohn, A.; Rochon, P. *Can. J. Chem.* **1998**, *76*, 1648.
(14) Lee, T. S.; Kim, D. Y.; Jiang, X. L.; Li, L.; Kumar, J.; Tripathy, S. *Macromol. Chem. Phys.* **1997**, *198*, 2279.
(15) Lee, T. S.; Kim, D. Y.; Jiang, X. L.; Li, L.; Kumar, J.; Tripathy, S. *J. Polym. Sci., Part A: Polym. Chem.* **1998**, *36*, 283.
(16) Xu, Z. S.; Drnoyan, V.; Natansohn, A.; Rochon, P. *J. Polym. Sci., Part A: Polym. Chem.* **2000**, *28*, 2245.
(17) Chen, J. P.; Labarthet, F. L.; Natansohn, A.; Rochon, P. *Macromolecules* **1999**, *32*, 8572.
(18) Köhler, W.; Robello, D. R.; Willand, C. S.; Williams, D. J. *Macromolecules* **1991**, *24*, 4589.
(19) Xu, C.; Wu, B.; Dalton, L.; Ranon, P. M.; Shi, Y.; Steier, W. H. *Macromolecules* **1992**, *25*, 6716.
(20) Natansohn, A.; Xie, S.; Rochon, P. *Macromolecules* **1992**, *25*, 5531.
(21) Barrett, C. J.; Natansohn, A.; Rochon, P. *J. Phys. Chem.* **1996**, *100*, 8836.
(22) Ho, M. S.; Natansohn, A.; Rochon, P. *Macromolecules* **1995**, *28*, 6124.
(23) Che, Y.; Sugihara, O.; Egami, C.; Fujimura, H.; Kawata, Y.; Okamoto, N.; Tsuchimoti, M.; Watanabe, O. *Jpn. J. Appl. Phys.* **1999**, *38*, 6316.

MA0102722